

UC San Diego

UC San Diego Previously Published Works

Title

Activation of G proteins by GIV-GEF is a pivot point for insulin resistance and sensitivity.

Permalink

<https://escholarship.org/uc/item/53q9c7c9>

Journal

Molecular biology of the cell, 26(23)

ISSN

1059-1524

Authors

Ma, Gary S
Lopez-Sanchez, Inmaculada
Aznar, Nicolas
et al.

Publication Date

2015-11-01

DOI

10.1091/mbc.e15-08-0553

Peer reviewed

Activation of G proteins by GIV-GEF is a pivot point for insulin resistance and sensitivity

Gary S. Ma^a, Inmaculada Lopez-Sanchez^a, Nicolas Aznar^a, Nicholas Kalogiropoulos^a, Shabnam Pedram^a, Krishna Midde^a, Theodore P. Ciaraldi^b, Robert R. Henry^b, and Pradipta Ghosh^{a,b,c}

^aDepartment of Medicine and ^cDepartment of Cell and Molecular Medicine, University of California, San Diego, School of Medicine, La Jolla, CA 92093; ^bDepartment of Veterans Affairs, VA San Diego Healthcare System, San Diego, CA 92161

ABSTRACT Insulin resistance (IR) is a metabolic disorder characterized by impaired insulin signaling and cellular glucose uptake. The current paradigm for insulin signaling centers upon the insulin receptor (InsR) and its substrate IRS1; the latter is believed to be the sole conduit for postreceptor signaling. Here we challenge that paradigm and show that GIV/Girdin, a guanidine exchange factor (GEF) for the trimeric G protein Gαi, is another major hierarchical conduit for the metabolic insulin response. By virtue of its ability to directly bind InsR, IRS1, and phosphoinositide 3-kinase, GIV serves as a key hub in the immediate postreceptor level, which coordinately enhances the metabolic insulin response and glucose uptake in myotubes via its GEF function. Site-directed mutagenesis or phosphoinhibition of GIV-GEF by the fatty acid/protein kinase C- θ pathway triggers IR. Insulin sensitizers reverse phosphoinhibition of GIV and reinstate insulin sensitivity. We also provide evidence for such reversible regulation of GIV-GEF in skeletal muscles from patients with IR. Thus GIV is an essential upstream component that couples InsR to G-protein signaling to enhance the metabolic insulin response, and impairment of such coupling triggers IR. We also provide evidence that GIV-GEF serves as therapeutic target for exogenous manipulation of physiological insulin response and reversal of IR in skeletal muscles.

Monitoring Editor

Asma Nusrat
Emory University

Received: Aug 4, 2015

Revised: Sep 2, 2015

Accepted: Sep 11, 2015

INTRODUCTION

Insulin resistance (IR) is a metabolic disorder in which adipocytes and muscle cells fail to take up and metabolize glucose in response to the hormone insulin. Although IR is a hallmark of type 2 diabetes mellitus (T2DM), IR alone in the absence of T2DM significantly increases the risk for stroke, heart failure, and atherosclerosis (Carter, 2005; Rundek *et al.*, 2010).

Although multiple etiologic factors contribute to the pathogenesis of IR (Saltiel and Kahn, 2001), they all ultimately converge to suppress critical components of metabolic insulin signaling. Insulin binds its receptors (InsR, IGF1R), triggering receptor autophosphorylation and subsequent tyrosine phosphorylation of insulin receptor substrate 1 (IRS1), among others. This leads to the recruitment and

This article was published online ahead of print in MBoc in Press (<http://www.molbiolcell.org/cgi/doi/10.1091/mbc.E15-08-0553>) on September 16, 2015.

Author contributions: G.S.M. and I.L.-S. designed, performed, and analyzed most of the experiments in this work, and S.P. assisted in key experiments. N.A. and N.K. designed, performed, and analyzed experiments on the interplay between GIV and IRS1. K.M. carried out FRET and dSTORM imaging. T.P.C. and R.R.H. provided access to well-characterized skeletal muscle biopsy samples from patients participating in clinical trials and provided expert guidance with design and execution of the patient-oriented research component of this work. G.S.M., I.L.-S., and P.G. wrote the manuscript. P.G. conceived, supervised, and funded the project.

Conflict of interest: The authors declare no competing financial interests.

Address correspondence to: Pradipta Ghosh (prghosh@ucsd.edu).

Abbreviations used: DAG, diacyl glycerol; DAPI, 4',6-diamidino-2-phenylindole; F.E., FRET efficiency; FRET, fluorescence resonance energy transfer; GAP, GTPase-activating protein; GDR, glucose disposal rate; GEF, guanine nucleotide exchange

factor; GLUT4, glucose transporter 4; GPCR, G protein-coupled receptor; GSV, GLUT4 storage vesicle; IB, immunoblotting; IgG, immunoglobulin G; IR, insulin resistance; IRS1, insulin receptor substrate 1; PA, palmitate; PCOS, polycystic ovarian syndrome; phocus-2nes, phosphorylation biosensors custom; PI3K, phosphoinositide 3 kinase; Pio, pioglitazone; PKC θ , protein kinase C- θ ; PM, plasma membrane; PTB, phosphotyrosine-binding domain; PTP, protein tyrosine phosphatase; RTK, receptor tyrosine kinase; SH2, Src homology 2; shRNA, short hairpin RNA; siRNA, small interfering RNA; T2DM, type 2 diabetes mellitus; TZDs, thiazolidinediones.

© 2015 Ma *et al.* This article is distributed by The American Society for Cell Biology under license from the author(s). Two months after publication it is available to the public under an Attribution-Noncommercial-Share Alike 3.0 Unported Creative Commons License (<http://creativecommons.org/licenses/by-nc-sa/3.0>).

"ASCB®," "The American Society for Cell Biology®," and "Molecular Biology of the Cell®" are registered trademarks of The American Society for Cell Biology.

activation of Src homology 2 (SH2) proteins such as p85 α (PI3-kinase) and downstream activation of Akt (Taniguchi *et al.*, 2006). Akt triggers the translocation of the 12-transmembrane glucose transporter 4 (GLUT4) to the plasma membrane (PM) by phosphoinhibiting the Rab GTPase-activating protein (GAP) AS160 (Miinea *et al.*, 2005). Among the many adaptors that relay signals within the insulin cascade, IRS1 is widely believed to serve as the major node for orchestrating metabolic insulin signaling (Taniguchi *et al.*, 2006).

Besides IRS1, metabolic insulin signaling also relies on the activation of heterotrimeric G proteins, another major hub in eukaryotic signal transduction. InsRs are functionally coupled to the pertussis toxin-sensitive G α i/o proteins, for example, insulin can trigger their activation (Rothenberg and Kahn, 1988; Ciaraldi and Maisel, 1989), localization (Gohla *et al.*, 2007), and phosphorylation (O'Brien *et al.*, 1987; Krupinski *et al.*, 1988). Activation of Gi augments insulin sensitivity (Chen *et al.*, 1997; Song *et al.*, 2001), enhances tyrosine phosphorylation of both InsR and IRS1 (Moxham and Malbon, 1996), and triggers efficient translocation of GLUT4 storage vesicles (GSVs) to the PM (Ciaraldi and Maisel, 1989; Kanoh *et al.*, 2000; Song *et al.*, 2001). Although multiple clues consistently point to a critical role of Gi activation in the insulin response, what couples and activates Gi downstream of InsR and how such activation may cross-talk with IRS1-dependent insulin signaling and trigger downstream metabolic events remain unknown. Additionally, little is known about how G-protein pathways are altered in IR.

With regard to the pathogenesis of IR, suppression of metabolic insulin signaling via the IRS1/PI3K pathway is an invariable hallmark (Kahn and Flier, 2000; Pessin and Saltiel, 2000; Le Roith and Zick, 2001). Such suppression occurs via common mechanisms that involve cellular accumulation of lipid metabolites (acyl-CoAs, ceramides, diacylglycerol, etc), which activate, among many other kinases, the critical protein kinase C- θ (PKC θ ; Griffin *et al.*, 1999; Yu *et al.*, 2002). PKC θ -dependent phosphoinhibition of IRS1 at Ser1-101 (Li *et al.*, 2004) is considered an important event that triggers lipid-induced IR. PKC θ expression levels are increased in the skeletal muscles of obese diabetics and hold an inverse relationship to insulin sensitivity (Schmitz-Peiffer *et al.*, 1997; Yu *et al.*, 2002), and PKC $\theta^{-/-}$ null mice demonstrate a protective effect against IR despite a high-fat diet (Kim *et al.*, 2004). These studies and many others have shaped the paradigm that IR is triggered when IRS1 is phosphoinhibited by kinases like PKC θ . However, some recent studies have revealed inconsistencies in this paradigm (summarized in Hoehn *et al.*, 2008). Emerging evidence indicates that IRS1 is insufficient for orchestrating the insulin response (Krook *et al.*, 1996) and that multiple receptor tyrosine kinases (RTKs) can trigger IR independent of IRS1 (Hoehn *et al.*, 2008). These studies raise the possibility that major unidentified signaling nodes exist within the insulin signaling cascade, whose inhibition via the fatty acid/PKC θ pathway triggers IR.

In this study, we define a single, multimodular signal transducer, GIV, as a critical node in metabolic insulin signaling. GIV is a guanine nucleotide exchange factor (GEF) that activates G α i1/2/3 (Garcia-Marcos *et al.*, 2009); contains a SH2-like domain that *directly binds* InsR (Lin *et al.*, 2014); is a direct substrate of InsR, which phosphorylates GIV at Y1764 (Lin *et al.*, 2011); is a bona fide enhancer of the PI3K-Akt pathway downstream of InsR and other RTKs (Lin *et al.*, 2011); and is a substrate for PKC θ . The latter phosphorylates and inhibits signaling via the GIV-G α i axis (Lopez-Sanchez *et al.*, 2013). Furthermore, a recent study has indicated that GIV may serve as a major regulator of the metabolic insulin response in skeletal muscle (Hartung *et al.*, 2013); overexpression of GIV in myoblasts leads to hyperphosphorylation of IRS1 and enhanced glucose uptake,

whereas depletion of GIV suppresses both. Despite these insights, the molecular mechanisms that enable GIV to enhance the metabolic insulin-IRS1 response in physiology or mechanisms that derail this pathway in the setting of IR remained unknown. On the basis of its ability to cross-talk with all these key mediators of metabolic insulin signaling, we asked whether GIV is a key determinant of insulin sensitivity in physiology and whether its phosphoregulation by PKC θ triggers IR.

RESULTS

Activation of G α i by GIV-GEF is required for glucose uptake in skeletal muscles

To determine the role of GIV-GEF in IR, we used differentiated L6 rat skeletal myotubes. Our rationale for this choice was guided by two facts: 1) although both adipocytes and skeletal muscles are sites for IR, full-length GIV is expressed more abundantly in skeletal muscles than in mature adipocytes (Uhlen *et al.*, 2010); and 2) a recent study showed that levels of expression of GIV mRNA in skeletal muscle biopsies from normal subjects tracks with insulin sensitivity, as measured by a hyperinsulinemic-euglycemic clamp (Hartung *et al.*, 2013). We found that depletion of GIV in L6 myotubes (by ~80–85%; Figure 1A) reduced the efficiency of glucose uptake by ~50% (Figure 1B), as determined by a well-established fluorometric assay (Yamamoto *et al.*, 2006). This defect was rescued by stably expressing small interfering RNA (siRNA)-resistant wild-type GIV (GIV-WT) but not the GEF-deficient F1685A mutant of GIV (GIV-FA), which can neither bind nor activate G α i (Garcia-Marcos *et al.*, 2009; Figure 1, C and D). It is noteworthy that the levels of stable expression of GIV-WT or mutants in GIV-depleted L6 myotubes were similar to the levels of endogenous GIV in these cells (Figure 1C), indicating that the effects observed are not merely due to overexpression of GIV at nonphysiological levels. These findings indicate that GIV is required for glucose uptake in skeletal muscles and that its GEF domain is essential.

Next we asked whether phosphoinhibition of GIV's GEF at Ser-1689 by PKC θ (Lopez-Sanchez *et al.*, 2013) also inhibits glucose uptake. We found that glucose uptake in cells expressing the constitutively phosphoinhibited S1689D mutant of GIV (GIV-SD) was half as efficient compared with those expressing GIV-WT (Figure 1, C and D), indicating that phosphoinhibition of GIV's GEF function by PKC θ impairs glucose uptake in response to insulin. These findings were reproduced in HeLa cells (Supplemental Figure S1), indicating that the effect of GIV-GEF we observe on glucose uptake may not be a restricted only to L6 myotubes but may represent a fundamental effect on IR.

To further pinpoint the impairment of Gi activation by GIV-GEF as the cause, we monitored glucose uptake in L6 myotubes stably expressing either wild-type (G α i3-WT) or a dominant-negative W258F mutant of G α i3, henceforth referred to as G α i3-WF (Figure 1E), which cannot bind or be activated by GIV but localizes and interacts with G β γ , G protein-coupled receptors (GPCRs), and G α i regulators similar to G α i3-WT (Garcia-Marcos *et al.*, 2010). We analyzed G α i3 (and not G α i1/2), because it is the most abundant G α i subunit expressed in skeletal muscles, as confirmed by proteomics (Hwang *et al.*, 2010). Glucose uptake was reduced in cells expressing G α i3-WF compared with those expressing G α i3-WT (Figure 1F), confirming that GIV drives efficient glucose transport after insulin stimulation via its ability to activate G α i proteins.

GIV binds ligand-activated InsR β and modulates multiple tiers of metabolic insulin signaling via its GEF function

To determine how GIV's GEF function affects the insulin signaling cascade, we analyzed key components of metabolic insulin signaling

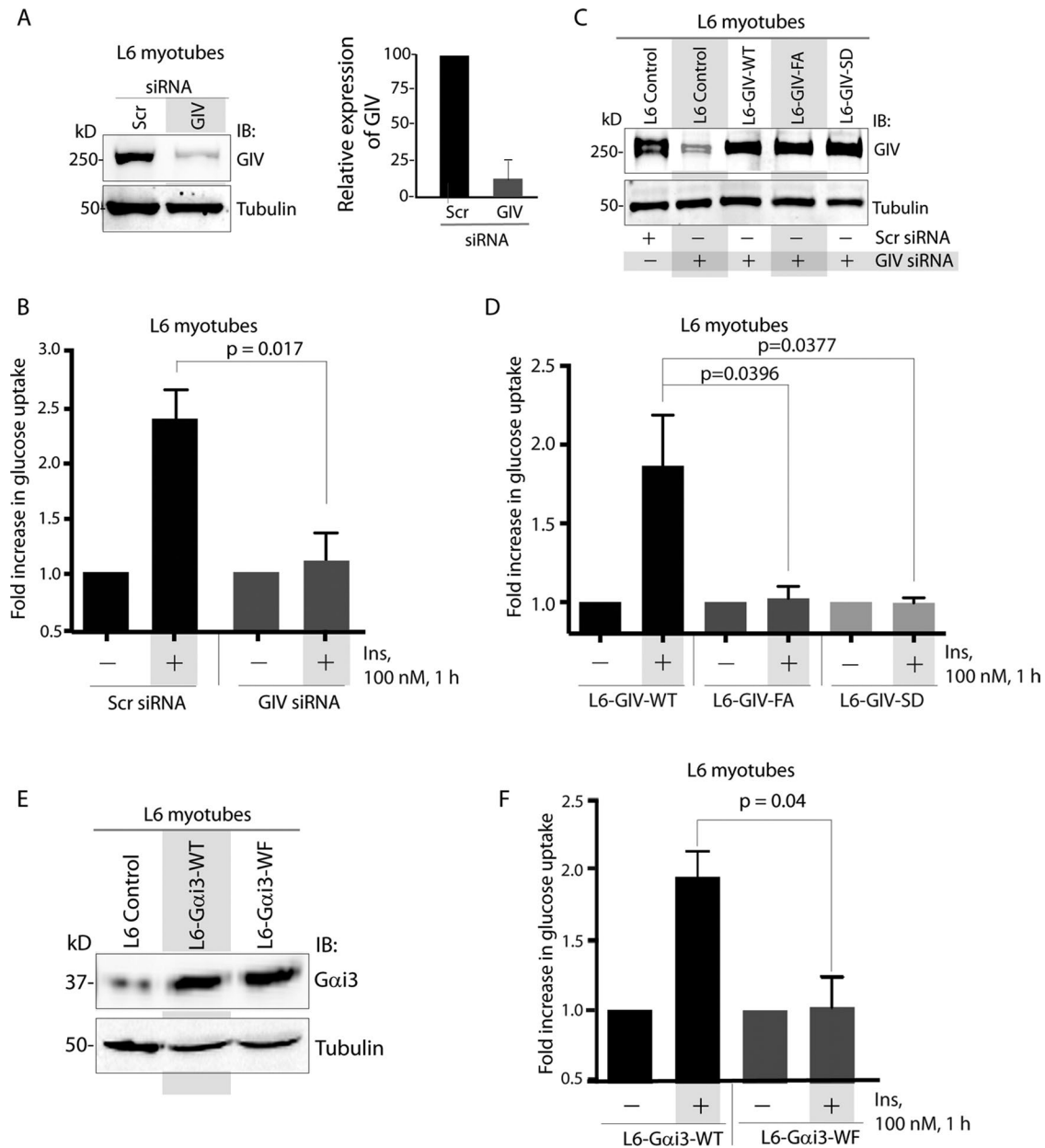


FIGURE 1: Activation of Gαi by GIV-GEF is essential for glucose uptake in skeletal muscles. (A) Left, lysates of L6 myotubes treated either with control (Scr) or with GIV siRNA were analyzed for GIV and tubulin by IB. Right, bar graph displays efficiency of GIV depletion. (B) Control (Scr siRNA) and GIV-depleted (GIV siRNA) L6 myotubes were analyzed for glucose uptake after insulin stimulation by fluorometric assay. Bar graphs display fold change in uptake compared with starved controls (y-axis). Error bars represent mean \pm SD; $n = 3$. (C) Control L6 myotubes or those stably expressing siRNA-resistant GIV-WT, GIV-FA, or GIV-SD were treated (+) or not (–) with either control (Scr) or GIV siRNA before lysis. Equal aliquots of whole-cell lysates were analyzed for GIV-FLAG expression by IB for GIV and tubulin. (D) L6 myotubes stably expressing siRNA-resistant GIV-WT, GIV-FA, or GIV-SD were depleted of endogenous GIV by siRNA as in C and analyzed for glucose uptake after insulin stimulation by fluorometric assay. Bar graphs display fold change in uptake compared with starved controls (y-axis). Error bars represent mean \pm SD; $n = 3$. (E and F) L6 myotubes stably expressing Gαi3-WT and Gαi3-WF were analyzed for Gαi3 and tubulin by IB (E) and for glucose uptake (F). Bar graphs display fold change in uptake compared with starved controls (y-axis). Error bars represent mean \pm SD; $n = 3$.

in L6 myotubes responding to insulin. Immunoblotting (IB) for phosphoproteins revealed that insulin triggers activation of GIV at 5 min, coincides with peak autophosphorylation of InsR β , and is followed by sustained phosphoactivation of IRS1 and Akt and phosphoinhibition of the GSV-associated Rab-GAP AS160 (Figure 2A); the latter is a key trigger step for exocytosis of GSVs (Miinea *et al.*, 2005). Activation of PKC θ was initiated by 5 min and sustained up to 30 min, and

inhibitory phosphorylation of GIV at S1689 by PKC θ peaked at 30 min. The time line of these events is consistent with the previously described role of this phospho event in the termination of GIV's GEF activity and disengaging GIV from Gαi (Lopez-Sanchez *et al.*, 2013). A similar analysis comparing L6 myotubes expressing GIV-WT or GIV-SD revealed that phosphoinhibition of GIV's GEF activity by PKC θ affects several of these key upstream events. Compared with

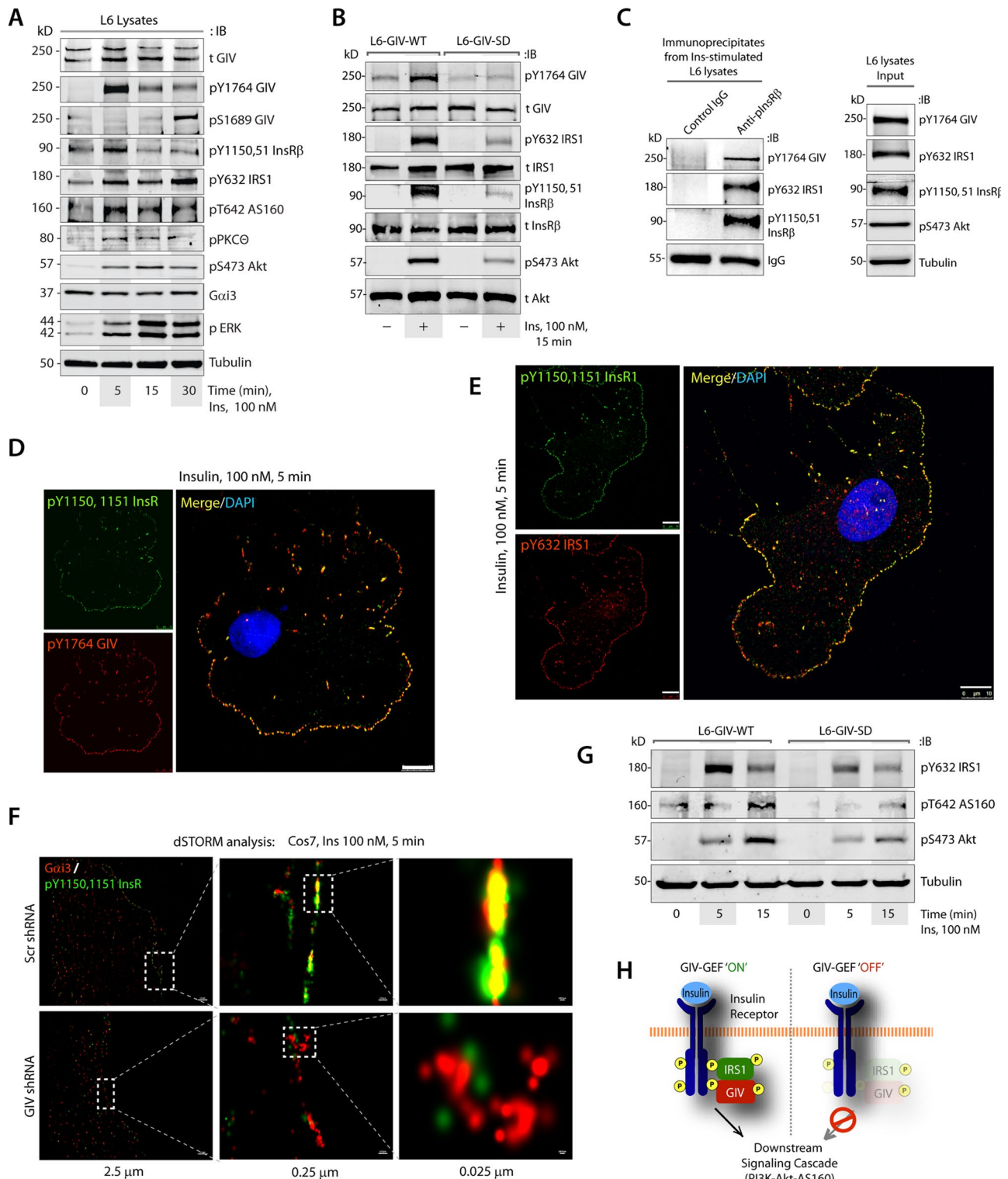


FIGURE 2: GIV-GEF binds and enhances autophosphorylation of InsR β and downstream metabolic insulin response. (A) Lysates of serum-starved L6 myotubes stimulated with insulin were analyzed for various components of metabolic insulin signaling by IB. (B) Lysates of serum-starved or insulin-stimulated L6 myotubes stably expressing GIV-WT or GIV-SD were analyzed for activation of GIV, IRS1, InsR β , and Akt by IB. (C) Immunoprecipitation was carried out on lysates (right) of insulin-treated L6 myotubes with anti-pInsR β or control immunoglobulin G (IgG). Bound immune complexes (left) were analyzed for activated GIV, IRS1, and InsR β by IB. (D and E) Serum-starved Cos7 cells were stimulated with insulin, fixed, and subsequently stained for active GIV (pY1764-GIV; red, D), active IRS1 (pY632-IRS1; red, E), active InsR β (pY1150/51-InsR β ; green), and 4',6-diamidino-2-phenylindole (DAPI)/DNA (blue). Scale bar: 10 μ m. (F) Serum-starved control (Scr shRNA) or GIV-depleted (GIV shRNA) Cos7 cells were stimulated with insulin, fixed, and stained for active InsR β (pY1150/51-InsR β ; green) and G α i3 (red) and analyzed by dSTORM microscopy. A high degree

L6-GIV-WT cell lines, global suppression of the insulin response was encountered in L6-GIV-SD cells, starting with the most upstream event, that is, suppressed autophosphorylation of InsR β at Y1150 and Y1151, which are essential for maximal phosphoactivation of substrate proteins (Flores-Riveros *et al.*, 1989; Figure 2B). At the immediate postreceptor level, phosphoactivation of GIV and IRS1 was suppressed, and Akt phosphorylation downstream was impaired (Figure 2B). Similar findings were noted also in paired HeLa-GIV-WT versus HeLa-GIV-SD cells (Supplemental Figure S2A).

Previous work showed that GIV's C-terminal SH2-like domain directly binds autophosphorylated cytoplasmic tails of multiple RTKs, including InsR β (Lin *et al.*, 2014; Midde *et al.*, 2015). In L6 myotubes, active GIV[pY1764] coimmunoprecipitated with ligand-activated InsR β -IRS1 complexes (Figure 2C). Active GIV[pY1764] also colocalized with the autophosphorylated InsR β at PM microdomains (Figure 2D), where activated IRS1 adaptors coexist (Figure 2E). These findings suggest that the InsR β -GIV-IRS1 complexes we observe in Figure 2C are likely assembled at the PM. To determine whether GIV links G α i proteins to ligand-activated InsR β at these PM microdomains, we used direct stochastic optical reconstruction microscopy (dSTORM). This mode of imaging achieves a spatial resolution of ~ 25 nm, and a high degree of colocalization between endogenous proteins indicates they are likely to interact (Huang *et al.*, 2010). In control cells, but not in GIV-depleted cells, G α i3 and ligand-activated InsR β showed a high degree of colocalization along the PM (Figure 2F, yellow pixels), indicating that active InsR β and G α i3 come within proximity to each other exclusively in the presence of GIV-GEF. As expected, the impairment of autophosphorylation of InsR β in GEF-deficient L6-GIV-SD mutant cells was also accompanied by defects in downstream activation of Akt and phosphoinactivation of its target Rab-GAP, AS160 (Figure 2G and Supplemental Figure S2B). Taken together, these results demonstrate that GIV binds to ligand-activated InsR β -IRS1 complexes on microdomains at the PM and links G α i to such complexes. The presence or absence of a functional GIV-GEF, via which GIV links and activates Gi in the vicinity of RTKs, appears to be a key determinant of whether multiple tiers within the metabolic insulin signaling cascade are activated maximally, beginning with the autophosphorylation and activation of InsR β (Figure 2H).

GIV directly binds and modulates the localization and functional phosphorylation of IRS1

Next we investigated how GIV may affect the phosphorylation/activation of IRS1, which is a major adaptor for the metabolic insulin responses. Because the hypophosphorylation of IRS1 observed by immunoblotting lysates of L6 myotubes and HeLa cells expressing the GEF-deficient SD phosphomimetic mutant does not provide enough information about the spatial and temporal dynamics of IRS1 phospho-dephosphorylation in cells, we used a genetically encoded fluorescent biosensor, phocus-2nes (Sato *et al.*, 2002) in fluorescence resonance energy transfer (FRET) studies. This biosensor shows energy transfer only when Y941 on IRS1 is phosphorylated and presents a docking site for the N-SH2 domain of p85 α (PI3K), thereby providing a readout of the function of such phosphorylation (Figure 3A). In cells expressing GIV-WT, we observed a significant

increase in FRET efficiency at/near the PM (F.E. 0.34 ± 0.08) within 5 min after insulin stimulation; however, in cells expressing GIV-SD, that response was blunted (F.E. 0.06 ± 0.03 ; Figure 3, B and C, and Supplemental Figure S3A), confirming that phosphoinhibition of GIV-GEF impairs functional phosphorylation of IRS1 at the PM. Because functional phosphorylation of IRS1 involves several steps, we asked whether GIV is required for the two earliest ones, that is, translocation of IRS1 from cytosol to the PM and its subsequent phosphorylation at that location in response to insulin. Compared with control cells, both steps were impaired in GIV-depleted cells (Figure 3, D and E, and Supplemental Figure S3, B and C). Coimmunoprecipitation studies on control or GIV-depleted cells further confirmed that recruitment of IRS1 to the activated InsR β was impaired in the absence of GIV (Figure 3F). To further pinpoint whether GIV's GEF function is essential for the recruitment of IRS1 to ligand-activated InsR, we first looked for insulin-triggered translocation of IRS1 from the cytosol to the PM in Cos7 cells expressing WT or SD GIV mutant (Supplemental Figure S3D). We found that IRS1 localized to the PM in cells expressing GIV-WT exclusively after ligand stimulation, whereas localization at the PM was suppressed in cells expressing GIV-SD. Next we analyzed receptor-bound complexes by immunoprecipitation assays in GIV-depleted HeLa cells stably expressing WT or SD GIV mutant (Figure 3G). In HeLa-GIV-WT cells, ligand stimulation triggered robust autophosphorylation of InsR (pY1150, 1151), which coincided with the recruitment of pYIRS1, GIV, and G α i3 (Figure 3G). Consistent with our prior observations in L6-GIV-SD cells (Figure 2B), autophosphorylation of InsR was suppressed also in HeLa-GIV-SD cells, and receptor-bound complexes (InsR-GIV-G protein or InsR-IRS1) were decreased. These results not only confirm the role of GIV's GEF function in enhancing the recruitment of IRS1 to ligand-activated InsR but also demonstrate the inhibitory effect of pS1689 GIV on both InsR-IRS1 and InsR-G α i3 complexes.

Because of the global effect of GIV depletion we observed on IRS1 localization, recruitment, and phosphoactivation, we next asked whether GIV binds IRS1. GIV coimmunoprecipitated with IRS1 before and after insulin stimulation (Figure 4A), indicating that the GIV-IRS1 interaction is constitutive. Pull-down assays with recombinant proteins showed that His-GIV-CT specifically bound the N-terminus of IRS1, demonstrating that the interaction is direct (Figure 4B). Furthermore, both WT and SD mutant GIV proteins bound IRS1 equally (Supplemental Figure S4, A and B), indicating that phosphorylation of GIV at S1689 by PKC θ does not impair GIV's ability to bind IRS1 and suggesting that GIV may bind IRS1 via a domain that is distinct from its GEF module. Despite the fact that GIV-SD retains its ability to bind IRS1, localization and activation of IRS1 were impaired in GIV-SD cells (Figure 3, B and C, and Supplemental Figure S3D), suggesting that the GIV-IRS1 interaction may serve a different role independent of the observed effects of phosphoinhibition of GIV-GEF on IRS1 signaling. We propose that the GIV-IRS1 interaction may serve as a scaffold for the stabilization of InsR β (RTK)/GIV/IRS1 ternary complexes at the PM, within which GIV's GEF function may modulate the phosphoactivation of IRS1 downstream of growth factors (Figure 4C).

of colocalization was observed, as determined by the presence of yellow pixels in the merged images. (G) Lysates of starved and insulin-stimulated L6 myotubes stably expressing GIV-WT or GIV-SD were analyzed for activation of IRS1, AS160, Akt, and tubulin by IB. (H) Schematic illustrating how the presence or absence of a functional GIV-GEF, via which GIV links and activates Gi in the vicinity of InsR β , dictates the intensity of metabolic insulin signaling, beginning with the activation and autophosphorylation of InsR β .

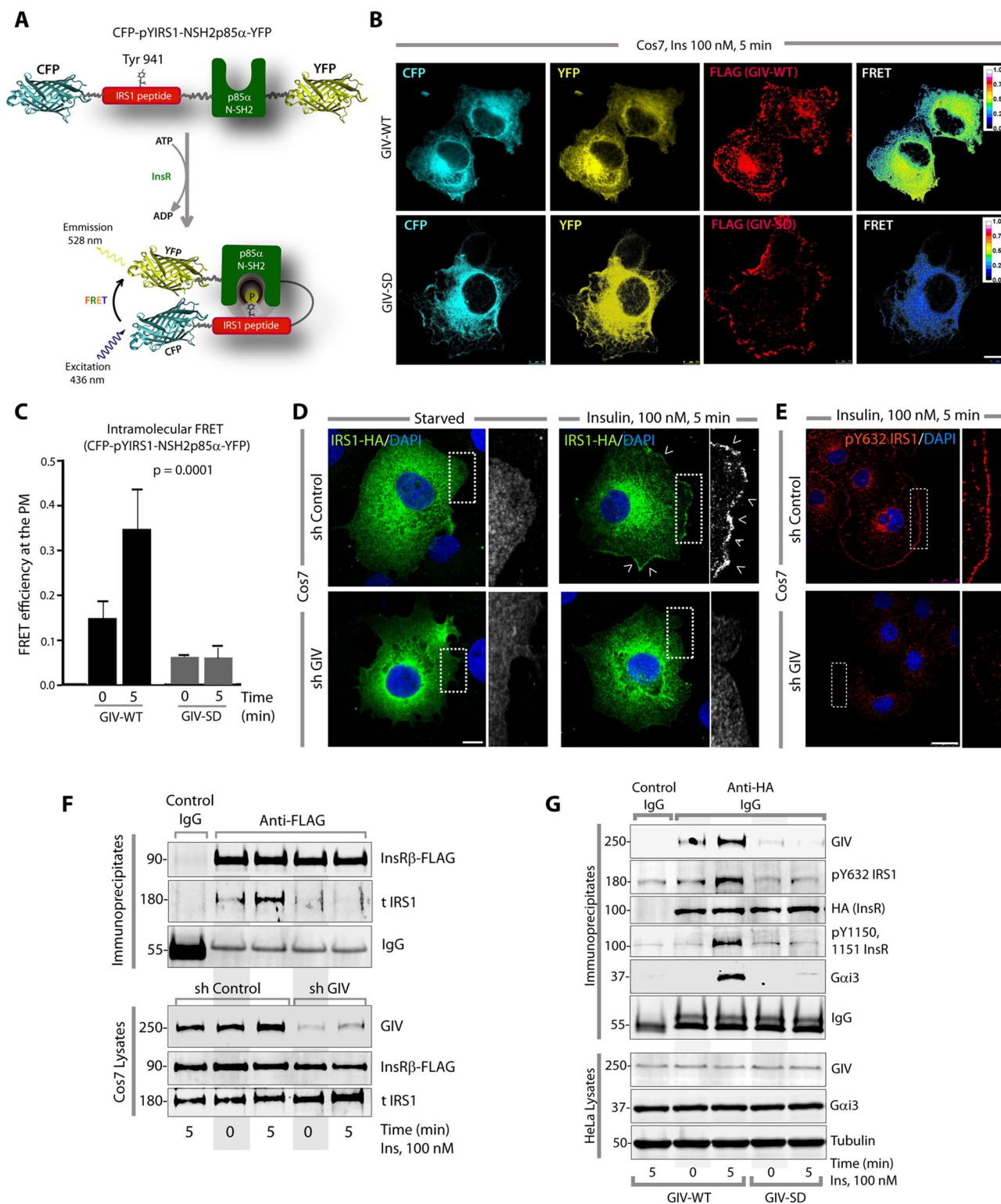


FIGURE 3: GIV-GEF directly binds and regulates the localization and activation of IRS1. (A) Schematic for the biosensor phocus-2nes is shown. Energy transfer from CFP to YFP occurs only when Y941 is phosphorylated and the N-SH2 domain of p85 α binds the phosphotyrosine ligand. (B and C) Serum-starved Cos7 cells coexpressing phocus-2nes with either GIV-WT-FLAG or GIV-SD-FLAG were stimulated with insulin, fixed, stained for FLAG (far red), and analyzed for FRET using confocal microscopy. Images panels display (from left to right, B) CFP, YFP, FLAG (GIV), and intensities of acceptor emission due to FRET in each pixel 5 min after insulin stimulation. Image panels of serum-starved (0 min) cells are shown in Supplemental Figure S3A. Bar graph (C) displays the FRET efficiency observed in GIV-WT versus GIV-SD cells at 0 and 5 min. The analysis represents five regions of interest from 4 to 6 cells/experiment (three independent experiments). Error bars = mean \pm SD. (D) Serum-starved control (sh Control) or GIV-depleted (sh GIV) Cos7 cells expressing IRS1-HA were stimulated with insulin, fixed, stained for HA (green) and DAPI/DNA (blue), and

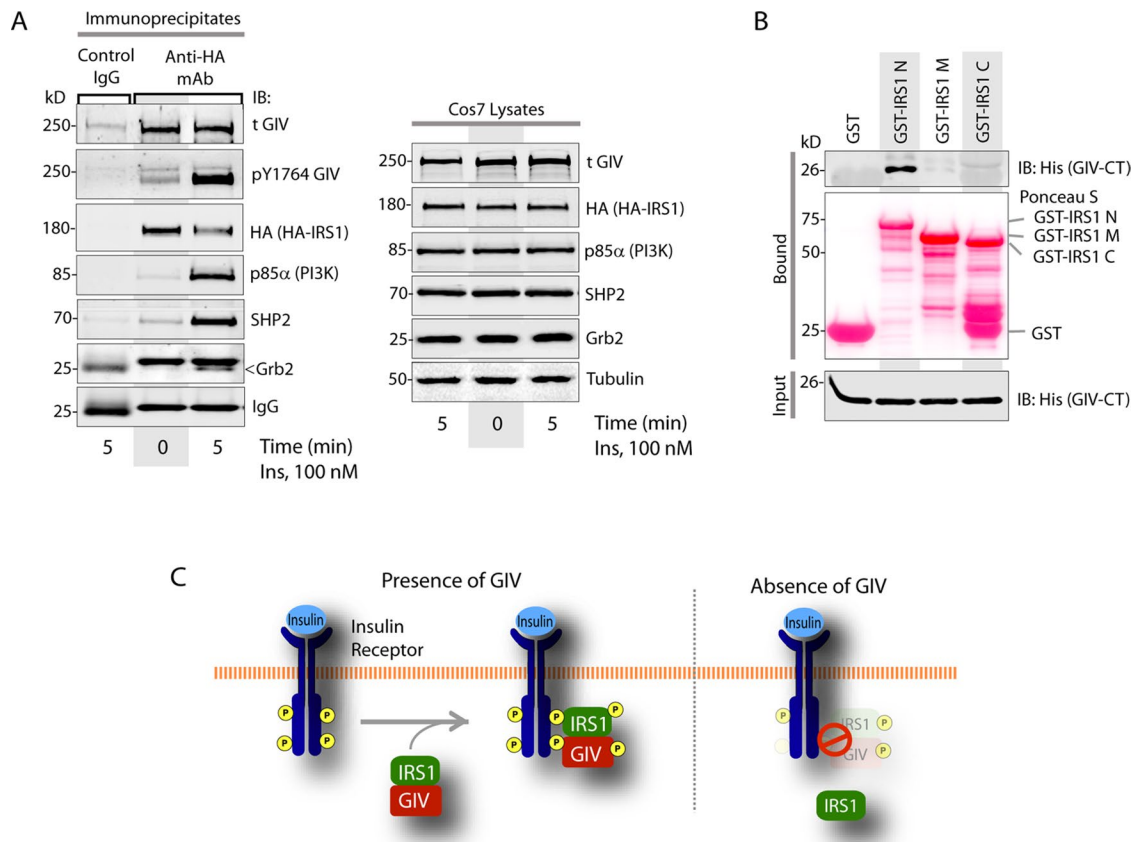


FIGURE 4: GIV directly and constitutively binds IRS1. (A) Immunoprecipitation was carried out on lysates (right) of starved or insulin-treated Cos7 cells expressing IRS1-HA. Lysates and bound immune complexes (left) were analyzed for activated GIV (pY1764-GIV), total (t)GIV, IRS1 (HA), p85 α , SHP2, and Grb2 by IB. (B) Pull-down assays were carried out with recombinant His-GIV-CT and GST-tagged domains of IRS1 (see the Supplemental Material) immobilized on glutathione beads. Bound (top) and input (bottom) proteins were analyzed for His-GIV-CT by IB with His mAb. (C) Schematic summarizing how the presence or absence of GIV affects localization and phosphoactivation of IRS1.

GIV-GEF is a target for the antagonist actions of fatty acids and insulin sensitizers

Because PKC θ is the kinase that orchestrates lipid-induced IR (Haasch *et al.*, 2006), we next asked whether fatty acids induce IR in part by phosphoinhibition of GIV-GEF at S1689 by PKC θ . When we induced IR in L6 cells using albumin-conjugated sodium palmitate (PA), which is known to activate PKC θ (Griffin *et al.*, 1999), we found that phosphorylation of GIV at S1689 was enhanced, GIV's ability to bind Gi was reduced, and phosphorylation of GIV at Y1764 was suppressed (Figure 5A and Supplemental Figure S5A), indicating that

PA induces phosphoinhibition of GIV-GEF and concomitantly suppresses tyrosine-based signaling via GIV. PA requires PKC θ to exert such phosphoinhibition, because inhibition of PKC θ abolished phosphoinhibition of GIV-GEF (Figure 5B). When PA-treated, insulin-resistant L6 cells were incubated with pioglitazone (Pio), an insulin sensitizer in the thiazolidinedione (TZD) class of drugs, phosphorylation of GIV at S1689 was reduced, and tyrosine phosphorylation of GIV was enhanced, indicating that Pio antagonized both the effects of PA and effectively reversed the phosphoinhibition of GIV-GEF by PKC θ (Figure 5A). Consistent with its role as a true insulin

analyzed by confocal microscopy. Insets show the magnification of the boxed regions. Scale bar: 10 μ m. Arrowheads denote PM. (E) Serum-starved control (sh Control) or GIV-depleted (sh GIV) Cos7 cells were stimulated with insulin, fixed, stained for endogenous pY632-IRS1 (red) and DAPI/DNA (blue), and analyzed by confocal microscopy. Insets show the magnification of the boxed regions. Scale bar: 10 μ m. (F) Immunoprecipitation was carried out on lysates of starved or insulin-stimulated control (sh Control) or GIV-depleted (sh GIV) Cos7 cells expressing InsR β -FLAG. Bound immune complexes were analyzed for IRS1, InsR β (FLAG), and IgG by IB. IRS1 coimmunoprecipitated with InsR β in control cells but not in GIV-depleted cells. (G) GIV-depleted HeLa cells stably expressing GIV-WT or GIV-SD were transiently transfected with InsR-HA, starved, and stimulated with 100 nM insulin for 5 min before lysis. InsR and receptor-bound complexes were immunoprecipitated by incubating equal aliquots of lysates with anti-HA mAb or contro IgG, followed by protein G beads. Immune complexes were analyzed for GIV, InsR (HA), ligand-activated InsR (pY1150, 1151 InsR), pY632 IRS1, and G α i3 by IB. Equal loading of lysates was confirmed by analyzing GIV, G α i3, and tubulin by IB. Maximal autophosphorylation of InsR and recruitment of GIV, IRS1, and G α i3 to the receptor was observed in cells expressing GIV-WT exclusively after insulin stimulation, but not in cells expressing GIV-SD.

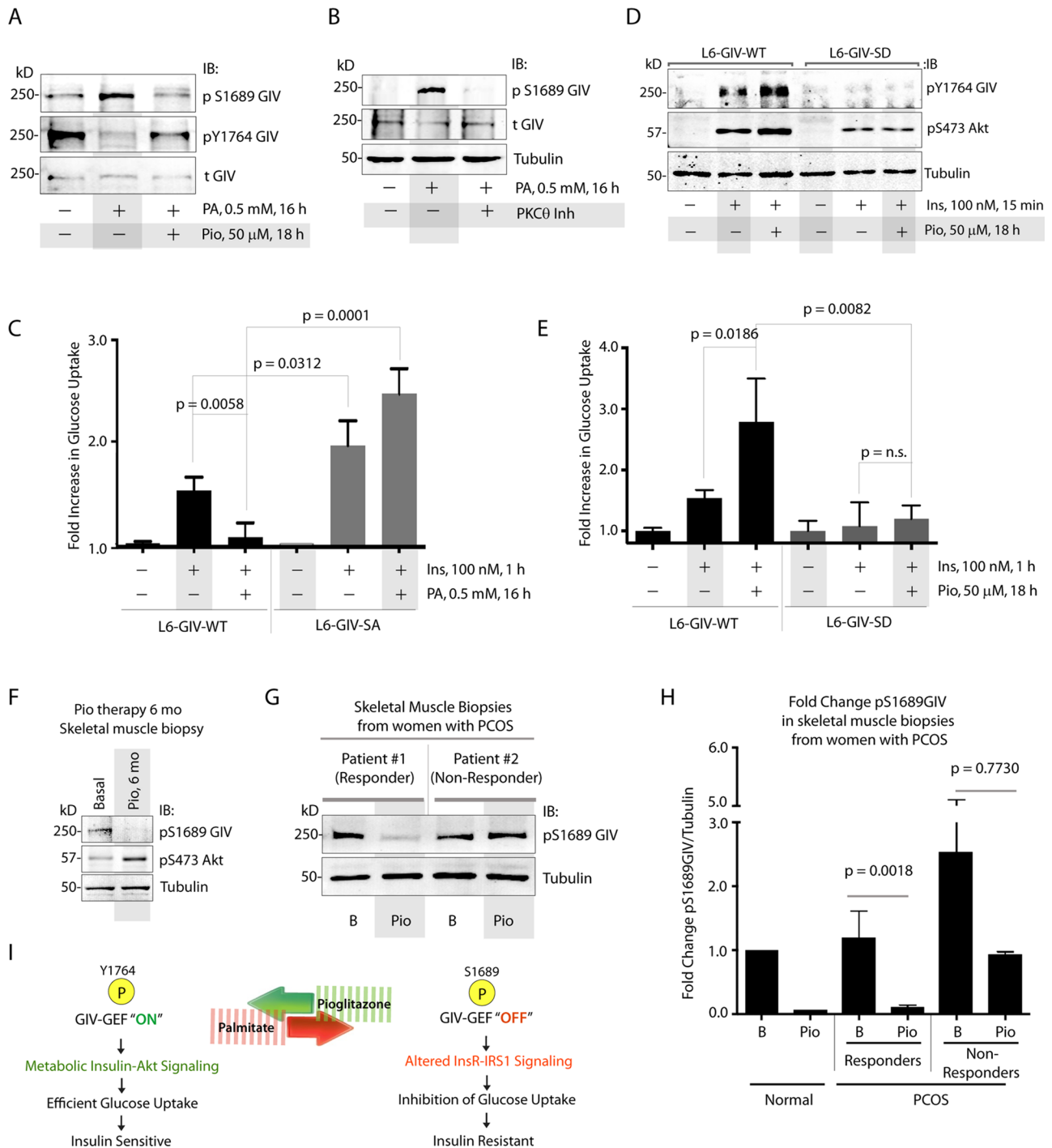


FIGURE 5: Phosphoinhibition of GIV-GEF by PKC θ is required for PA-induced IR and dephosphorylation of GIV-GEF is essential for the action of Pio. (A) Lysates of L6 myotubes treated (+) or not (–) with PA alone or a combination of PA and Pio were analyzed for phosphorylation of GIV at S1689 and Y1764 and total (t)GIV by IB. (B) Lysates of L6 myotubes treated (+) or not (–) with PA alone or a combination of PA and a pseudosubstrate PKC θ inhibitor were analyzed for phosphorylation of GIV at S1689 (pS1689 GIV), total (t)GIV, and tubulin by IB. (C) L6 myotubes stably expressing siRNA-resistant GIV-WT or GIV-SA were depleted of endogenous GIV by siRNA, treated with PA (+) or vehicle control (–), and subsequently analyzed for insulin-stimulated glucose uptake by fluorometric assay. Bar graph displays fold change in glucose uptake compared with starved controls (y-axis). Error bars represent mean \pm SD; $n = 3$. (D) L6 myotubes stably expressing siRNA-resistant GIV-WT or GIV-SD were depleted of endogenous GIV by siRNA, treated (+) or not (–) with Pio, and subsequently stimulated with insulin before lysis. Lysates were analyzed for activation of GIV (pY1764 GIV) and Akt (pS473Akt) by IB. (E) L6 myotubes stably expressing siRNA-resistant GIV-WT or GIV-SD were depleted of endogenous GIV by siRNA, treated (+) or not (–) with Pio, and subsequently analyzed for insulin-stimulated glucose uptake by fluorometric assay. Bar graph displays fold change compared with starved controls (y-axis). Error bars represent mean \pm SD; $n = 3$. (F) Equal aliquots of lysates of vastus lateralis muscle biopsies from obese T2DM subjects,

sensitizer that improves insulin action in peripheral tissues, Pio also enhanced tyrosine phosphorylation of GIV and Akt signaling triggered by insulin in insulin-sensitive L6 cells never exposed to PA (Supplemental Figure S5, B and C).

We then investigated whether phosphoinhibition of GIV-GEF by PKC θ in L6 myotubes plays a role in mediating the antagonistic effects of PA and Pio in the induction and reversal of IR, respectively. PA induced IR in L6-GIV-WT cells, as determined by a blunted glucose-uptake response to insulin (Figure 5C). However, L6 cells expressing a nonphosphorylatable GIV S1689A mutant (L6-GIV-SA) were resistant to PA, that is, these cells remained sensitive to insulin regardless of PA treatment and demonstrated higher glucose uptake compared with L6-GIV-WT cells (Figure 5C). These results demonstrate that the selective inhibition of GIV-GEF by PKC θ via phosphorylation of a single Ser-1689 is an essential mechanism by which PA triggers IR in L6 myotubes. As for Pio, we found that it reinstated insulin signaling in PA-treated, insulin resistant L6-GIV-WT cells, as determined by restored tyrosine phosphorylation of GIV and Akt signaling (Figure 5D and Supplemental Figure S5D). However, L6 cells expressing a constitutively phosphoinhibited GIV SD mutant (L6-GIV-SD) were resistant to Pio, that is, these cells showed no discernible enhancement of signaling compared with L6-GIV-WT cells (Figure 5D and Supplemental Figure S5D). Furthermore, Pio reversed the PA-induced IR state in L6-GIV-WT cells, but not in L6-GIV-SD cells, as determined by glucose uptake after insulin stimulation (Figure 5E). Because Pio is known to improve insulin sensitivity in muscle tissue in part by antagonizing the activity of protein kinases such as PKC θ (Markova *et al.*, 2010), our results demonstrate that reversal of phosphoinhibition of GIV-GEF by PKC θ on Ser-1689 is an essential mechanism via which Pio reverses IR and sensitizes L6 myotubes to the action of insulin. The inability to reverse such phosphoinhibition (as in the case of the GIV-SD mutant, which mimics a constitutive phosphoinhibited state) makes cells nonresponsive to the insulin-sensitizing actions of Pio.

The physiological significance of these observations in cultured L6 myotubes was confirmed by findings in patients with IR, in whom chronic treatment with Pio reduced the phosphoinhibition of GIV-GEF and enhanced phosphorylation of Akt in skeletal muscles (vastus lateralis) of obese T2DM patients (Figure 5F). Moreover, patients with polycystic ovarian syndrome (PCOS) in whom IR was clinically reversed by Pio therapy, that is, responders (as determined by 24-h glucose levels and glucose disposal rate [GDR] determined by a hyperinsulinemic–euglycemic clamp) showed a significant reduction in phosphoinhibition of GIV at S1689 in their muscles. By contrast, PCOS patients who failed the Pio treatment trial (i.e., nonresponders) had high pretreatment and/or posttreatment levels of phosphoinhibition of GIV-GEF (Figure 5, G and H). Taken together, our results demonstrate that a single phospho event (PKC θ -dependent phosphorylation of GIV at S1689), which selectively inhibits GIV-GEF and

therefore abolishes activation of Gi by GIV, is a common pivot point for both PA and Pio to exert their antagonistic actions in IR. Phosphorylation at S1689 is essential for PA to induce IR, whereas dephosphorylation is required for Pio to enhance tyrosine phosphorylation of IRS1 and GIV, restore Akt signaling, and reinstate insulin sensitivity (Figure 5I).

Cell-permeant GIV-derived peptides can effectively reverse IR in skeletal muscle

We next asked whether GIV-GEF can serve as a therapeutic target for exogenous modulation of IR. To investigate this, we used recently validated recombinant, cell-permeant TAT-tagged GIV-CT peptides (WT and GEF-deficient FA mutant peptides spanning GIV's GEF and SH2-like domains; Figure 6, A and B). These peptides offer a nongenetic approach for exogenous manipulation of GIV-GEF-dependent signaling programs and cellular phenotypes in diverse cells and a variety of pathophysiological processes (Ma *et al.*, 2015). L6 myotubes homogeneously took up TAT peptides (~90% efficiency of uptake; Figure 6C). Uptake of GIV-CT-WT peptides was associated with enhancement of stress-fiber formation and phosphorylation of IRS1 and Akt proteins in response to insulin (Figure 6, C and D). However, uptake of GIV-CT-FA peptides disrupted the actin stress fibers, as shown previously in other cell lines, and suppressed IRS1 and Akt phosphorylation in response to insulin. Consistent with these signaling programs, insulin-stimulated glucose uptake in the basal state was unaffected by GIV-CT-WT peptides but was significantly inhibited by GIV-CT-FA peptides (Figure 6E). GIV-CT-WT, but not the FA mutant peptides, effectively reversed PA-induced IR (Figure 6F), and ~800 nM of WT peptide was as effective as 50 μ M Pio in reversing such IR (Figure 6G). These studies demonstrate that cell-permeant GIV-CT peptides can enhance metabolic insulin signaling and reverse IR effectively in a GEF-dependent way.

DISCUSSION

Phosphoinhibition of GIV-GEF by PKC θ triggers lipid-induced IR; dephosphorylation of GIV-GEF reinstates insulin sensitivity

The fundamental discovery in this work is that GIV-GEF plays a major role as a dominant conduit for insulin response in the skeletal muscle, and identification of key phospho events that allow this GEF to serve as a decisive pivot/node for cellular insulin response in physiology and disease (see Figure 7). In lean individuals, insulin triggers activation of GIV by tyrosine phosphorylation (pY), GIV's GEF function is turned "on," and G α i is activated, metabolic insulin signaling is initiated through the InsR/IRS1/PI3K/Akt signaling axis, culminating in efficient exocytosis of GSVs and subsequent uptake of glucose. In the obese, circulating free fatty acids trigger the accumulation of diacyl glycerol (DAG) and activation of PKC θ in skeletal muscle, which in turn phosphorylates GIV's GEF motif at S1689

obtained before (basal) or after 6 mo of Pio therapy, were analyzed for phosphoinhibition of GIV-GEF (pS1689 GIV) and phospho Akt (pS473 Akt) by IB. Representative samples are shown ($n = 8$). (G and H) Equal aliquots of lysates of vastus lateralis muscle biopsies from patients with PCOS, obtained before (basal) and after Pio therapy, were analyzed for pS1689GIV by IB. (G) A representative immunoblot of biopsies obtained from "responder" and "nonresponder" patients are shown ($n = 8$). Bar graph displays fold change in GIV phosphorylation at S1689 observed in normal and PCOS patients before and after Pio treatment (y-axis) (H). B, basal; Pio, pioglitazone treatment. Error bars represent mean \pm SD. (I) Schematic illustrates our proposed model for GIV's role as a pivot for the antagonistic actions of fatty acids like palmitate that trigger IR (red arrow) and insulin sensitizers like Pio that reverse IR (green). Phosphorylation at S1689 is essential for PA to induce IR, whereas dephosphorylation is required for Pio to enhance tyrosine phosphorylation of IRS1 and GIV, restore Akt signaling, and reinstate insulin sensitivity.

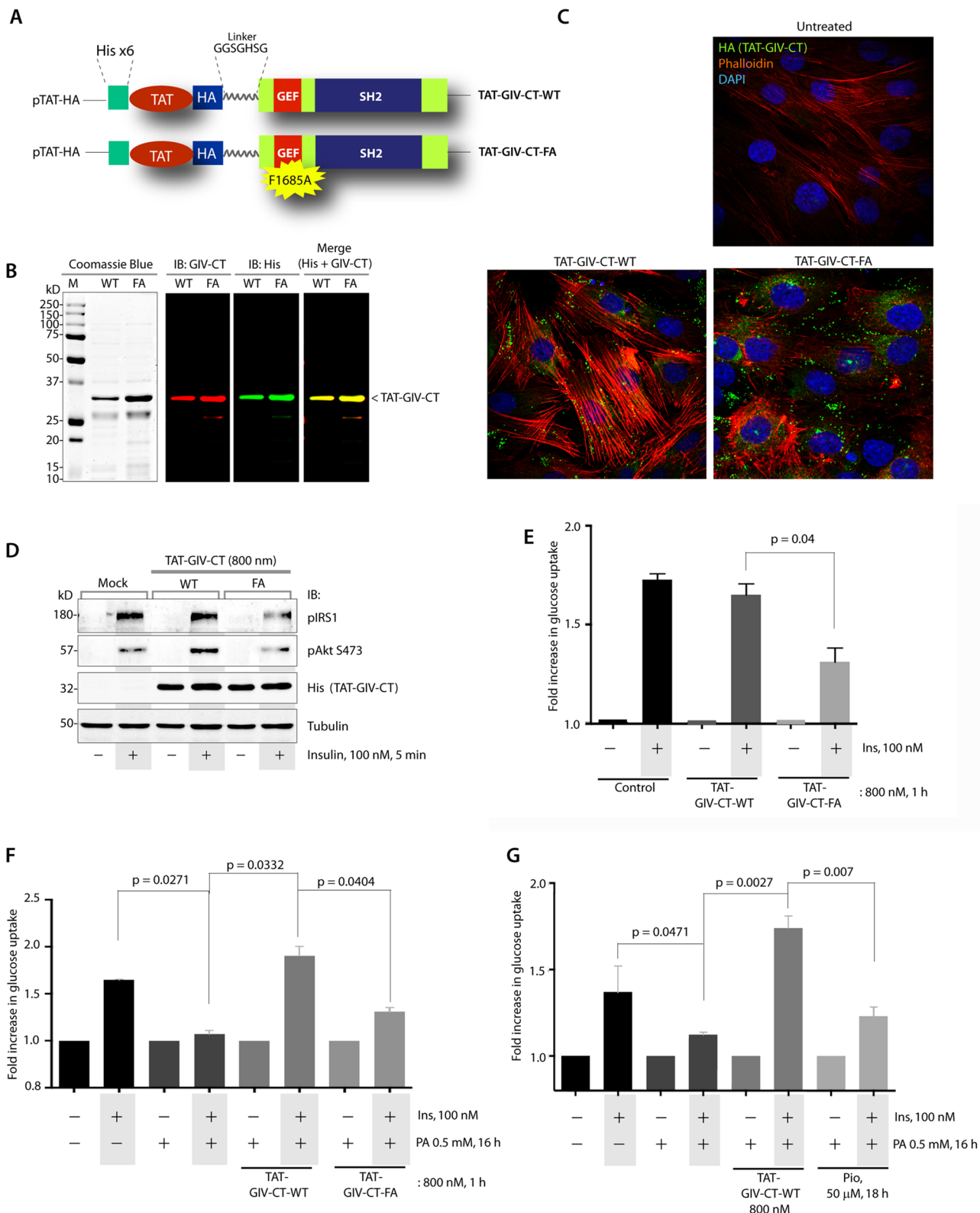


FIGURE 6: Cell-permeant TAT-GIV-CT-WT peptides, but not FA mutant peptides, effectively reverse lipid-induced IR in skeletal muscles. (A) Design of the cell-permeant TAT-GIV-CT peptides is shown. TAT-PTD was fused to His and HA tags and coupled via a linker (GGSGHSG) to the C-terminus of GIV (aa 1660–1870). (B) Purified recombinant TAT-GIV-CT peptides were analyzed by Coomassie blue staining and by IB with anti GIV-CT and anti-His antibodies. (C) L6 myotubes were treated with TAT-GIV-CT-WT or FA peptides and cultured overnight in low serum conditions (0.2% fetal bovine serum) before fixation. Fixed cells were stained for His (green), phalloidin (F-actin, red), and DAPI/DNA (blue) and analyzed by confocal microscopy. (D) L6 myotubes were treated with TAT-GIV-CT-WT or FA peptides, starved, and stimulated with insulin before lysis. Equal aliquots of lysates were analyzed for transduction of TAT-peptides with anti-His antibody, activation of IRS1 (pY632-IRS1) and Akt (pS473) by IB. (E) L6 myotubes were treated with

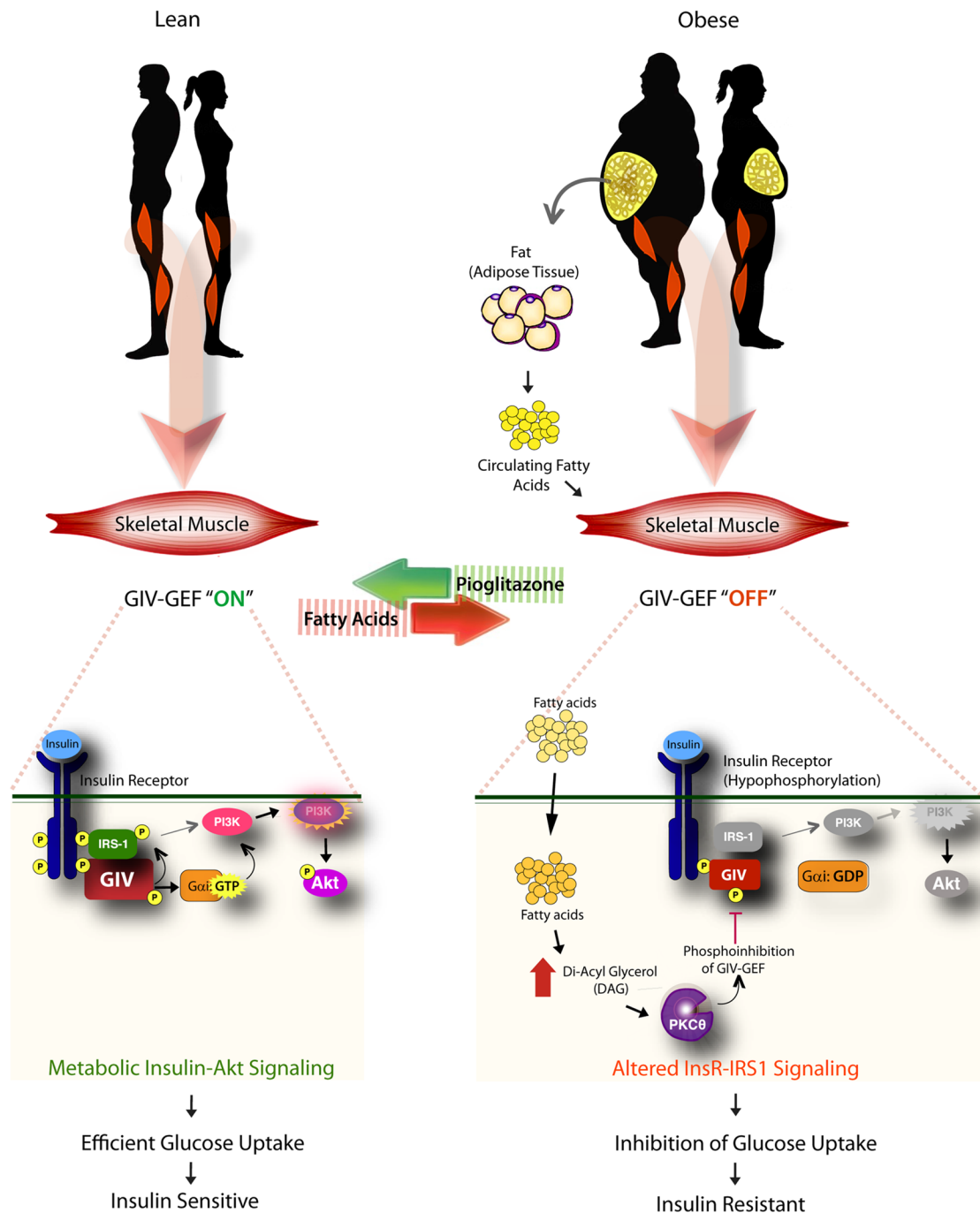


FIGURE 7: Schematic summarizing how GIV-GEF is a pivotal node for metabolic insulin response in lean normals (left) and for lipid-induced IR in the obese (right). Left, in lean individuals, insulin triggers tyrosine phosphorylation and activation of GIV (pY1764), GIV's GEF function is "on" and Gαi is activated. Metabolic insulin signaling is enhanced through the InsR/IRS1/PI3K/Akt/AS160 signaling axis, resulting in efficient exocytosis of GSVs and rapid uptake of glucose. Right, in the obese, circulating free fatty acids trigger the accumulation of DAG, and PKCθ is activated. PKCθ phosphorylates GIV at S1689 and turns "off" its GEF function. Consequently, Gαi remains inactive, and the InsR/IRS1/PI3K/Akt/AS160 signaling cascade is suppressed, thereby triggering IR.

TAT-GIV-CT-WT or FA peptides, starved, and subsequently analyzed for insulin-stimulated glucose uptake by fluorometric assay. Bar graph displays fold change in uptake compared with starved controls (y-axis). Error bars represent mean \pm SD. (F) L6 myotubes were treated (+) or not (–) with PA to induce IR, then transduced with TAT-GIV-CT-WT or FA peptides, and subsequently analyzed for insulin-stimulated glucose uptake by fluorometric assay. Bar graph displays fold change in uptake compared with starved controls (y-axis). Error bars represent mean \pm SD. (G) L6 myotubes were treated (+) or not (–) with PA to induce IR, then either treated with Pio or transduced with TAT-GIV-CT-WT peptides (as indicated), and subsequently analyzed for insulin-stimulated glucose uptake by fluorometric assay. Bar graph displays fold change in uptake compared with starved controls (y-axis). Error bars represent mean \pm SD.

and selectively turns “off” the GEF function. Consequently, G α i remains inactive, and a majority of the key elements of metabolic insulin signaling are suppressed, thereby triggering IR.

We also provide evidence that reversible phosphorylation of GIV at S1689 by PKC θ and the ability of this single phospho event to modulate the InsR-GIV-G α i signaling axis are critical determinants of cellular insulin responses. We demonstrated that this phospho event alone is *sufficient* to mimic fatty acid-induced IR and that fatty acids *require* such phosphorylation to induce IR. Although this study dissected the interplay between GIV and PKC θ in lipid-induced IR, because GIV can intercept signaling downstream of multiple classes of receptors (GPCRs and RTKs) and non-RTKs alike (reviewed in Garcia-Marcos *et al.*, 2015) and is an enhancer of STAT3 as well as its transcriptional target (Dunkel *et al.*, 2012), it is possible that GIV is a central node for other major triggers of IR, that is, inflammation, suppression of adiponectin, leptin resistance, and so on, which also require activation of PKC θ (Itani *et al.*, 2000; Lin *et al.*, 2000; Shulman, 2000; Anderson *et al.*, 2006) and/or the JAK-STAT3 pathway (Mashili *et al.*, 2013; Wunderlich *et al.*, 2013).

We also show that TZDs like Pio release the phosphoinhibition on GIV-GEF and restore its function. Such restoration was essential for TZD action, because TZDs failed to reverse IR and reinstate insulin sensitivity in cells expressing the constitutively phosphomimic GIV-S1689D mutant. Because chronic TZD therapy does not suppress PKC θ (Markova *et al.*, 2010), the reduction in levels of GIV phosphorylation at S1689 we observed after TZD therapy is likely to be a consequence of dephosphorylation by one of the many S/T phosphatases that are activated by TZDs in a PPAR γ -dependent manner (Altioik *et al.*, 1997; Pugazhenthii and Khandelwal, 1998; Sharma *et al.*, 2004; Cho *et al.*, 2006). Regardless of the mechanism(s) involved, our results indicate that GIV is a major target of TZDs that can account, in part, for TZD action on skeletal muscle. We conclude that reversible phosphorylation at S1689 and inhibition of the GEF function, via which GIV activates G α i, serves as a molecular switch for flipping skeletal muscles between insulin-sensitive and insulin-resistant states. Because GIV specifically binds G α i and not G α q/11 (Le-Niculescu *et al.*, 2005), these findings do not account for the previously described role of yet another G protein, G α q/11, in insulin response (Imamura *et al.*, 1999).

GIV's GEF function modulates several tiers within the metabolic insulin signaling cascade

We demonstrated that activation of G α i by GIV impacts many tiers within the insulin signaling cascade and that phosphoinhibition of GIV's GEF function antagonizes them all. We previously showed that GIV directly binds autophosphorylated cytoplasmic tails of ligand-activated InsR via its C-terminal SH2-like module (Lin *et al.*, 2014). Both the SH2-like module and GIV's GEF functions are critical for coupling of G proteins to ligand-activated InsR (Garcia-Marcos *et al.*, 2011; Lin *et al.*, 2014; Midde *et al.*, 2015). We show here that, at the level of the receptor, activation of G α i via GIV's GEF motif is required for maximal autophosphorylation and activation of InsR β and recruitment and phosphoactivation of its major substrate, IRS1. The sites of autophosphorylation on InsR β that GIV enhanced, Y1150 and Y1151, are required for maximal activation of the InsR β kinase (White *et al.*, 1988), and a failure to activate InsR β kinase in skeletal muscles has been implicated in IR (Maegawa *et al.*, 1991; Nolan *et al.*, 1994; Goodyear *et al.*, 1995). Although it is unclear how activation of G α i by GIV may enhance receptor autophosphorylation, it is not entirely surprising, because activation of G α i has previously been implicated in the enhancement of InsR autophosphorylation (Kreuzer *et al.*, 2004) and because we previously showed that

activation of G α i by GIV's GEF function can similarly enhance autophosphorylation of yet another RTK, EGFR (Ghosh *et al.*, 2010). In both instances, suppression of protein tyrosine phosphatases (PTPs) has been implicated as the mechanism for enhanced receptor autophosphorylation (Moxham and Malbon, 1996; Lin *et al.*, 2014). Because GIV directly binds ligand-activated InsR β (Lin *et al.*, 2014) and triggers the formation of InsR β -G α i complexes at the PM, it is possible that the formation of such InsR β -GIV-G α i complexes suppresses the recruitment and/or activation of key PTPases. We conclude that the GIV-G α i axis enhances cellular insulin response by increasing InsR β kinase activity and autophosphorylation, two upstream events in insulin signaling.

At the immediate postreceptor level, we demonstrate that GIV binds and modulates the functions of IRS1. Activation of G α i by GIV enhanced the recruitment of IRS1 to the ligand-activated receptors at the PM, triggered robust tyrosine phosphorylation at Y632 and Y941 on IRS1, and enhanced the formation of IRS1-p85 α (PI3K) complexes. Unlike the ligand-dependent nature of InsR β -GIV or InsR β -IRS1 (Sun *et al.*, 1991) interactions, the GIV-IRS1 interaction was constitutive. We also provide evidence that this binding was direct and that it involved the C-terminal region of GIV and the N-terminal region of IRS1. The latter contains a phosphotyrosine-binding domain (PTB) that is responsible for the direct interaction of IRS1 with InsR β (Eck *et al.*, 1996). Our findings of InsR β -GIV-IRS1 complexes upon insulin stimulation suggest that GIV may bind IRS1 at a distinct site where the autophosphorylated cytoplasmic tail of InsR β docks within the PTB. The enhanced recruitment of IRS1 to InsR β in the presence of GIV suggests that GIV may serve as a signal amplifier at the immediate postreceptor level by facilitating the recruitment of more IRS1 adaptors per activated InsR. Based on recent experimental evidence that questions the exclusivity of IRS1 for InsR β (Knowlden *et al.*, 2008) and that shows GIV is capable of binding multiple RTKs (e.g., EGFR, PDGFR, VEGFR; Lin *et al.*, 2014; Lopez-Sanchez *et al.*, 2014), it is possible that GIV provides the necessary molecular basis for IRS1 to serve as a common conduit for metabolic response observed downstream of receptors other than InsR β .

Although the precise mechanism of GIV-IRS1 interaction remains uncertain, this interaction adds GIV to the lengthy list of proteins that IRS1 scaffolds within the insulin signaling cascade (White, 2006). The finding that GIV enhanced tyrosine phosphorylation of IRS1 is consistent with the concomitant increase in the kinase activity of InsR β and enhanced recruitment of IRS1 to the PM, the latter is a prerequisite for maximal tyrosine phosphorylation of IRS1 (Myers *et al.*, 1995; Voliovitch *et al.*, 1995). We conclude that GIV is required for maximal PM recruitment and tyrosine phosphorylation of IRS1, both key events implicated in metabolic insulin signaling via IRS1. In doing so, and by virtue of its ability to directly bind and bring together several other components of the metabolic insulin response (InsR, IRS1, G proteins, actin, PI3K, Akt), GIV serves as an integral hub at the immediate postreceptor that fine-tunes IRS1-dependent metabolic insulin signaling.

Further downstream, the PI3K-Akt signaling pathway was maximally enhanced in the presence of an intact GIV-GEF, and a major pathway downstream of Akt was triggered, that is, phosphoinhibition of the Rab-GAP AS160. Prior studies have demonstrated that docking of GSVs at the PM requires activation of Rab proteins (Miinea *et al.*, 2005; Sun *et al.*, 2010; Lansey *et al.*, 2012) in response to insulin (Bai *et al.*, 2007). By triggering the phosphoinhibition of Rab-GAP AS160, GIV's GEF function is likely to affect the exocytosis of GSVs via potentiation of Rab GTPases. We conclude that GIV functionally interacts with and enhances key signaling

events that can also coordinate membrane trafficking within the insulin response cascade, and in doing so, it delineates a molecular basis for the observed engagement between these events during insulin-triggered glucose uptake into cells (Leto and Saltiel, 2012).

Although this study has specifically dissected the role of GIV's GEF function in coordinating key signaling events that comprise the metabolic insulin response, it is notable that the GEF motif merely represents a stretch of ~30–35 aa within a 1871-aa-long, multimodular protein made up of several other key functional modules that may take part in other key aspects of glucose uptake. One such well-defined module is GIV's SH2-like domain, which is necessary and sufficient for GIV to directly bind the autophosphorylated cytoplasmic tail of InsR; without a functional SH2-like domain, GIV can neither bind InsR nor facilitate the formation of InsR–G protein complexes (Lin *et al.*, 2014). Another such module, whose boundaries remain to be defined, but which appears to be functionally distinct from the GEF module, is a region within GIV's C-terminus that directly binds IRS1 (Figure 4B); it is possible that selective inhibition of GIV–IRS1 interaction may also impair the metabolic insulin response and glucose uptake. Our own recent findings that GIV regulates cargo trafficking from the ER–Golgi intermediate compartment (ERGIC) to the Golgi (Lo *et al.*, 2015) raises the possibility that GIV may also play a role in regulating GLUT4 trafficking from the Golgi to GSVs. Additionally, GIV is also known to regulate clathrin-mediated endocytosis and endocytic trafficking (Beas *et al.*, 2012; Weng *et al.*, 2014), two processes closely intertwined with and key determinants of the kinetics of GLUT4 trafficking, glucose uptake, and down-regulation of insulin receptor signaling. Because the actin cytoskeleton has also been described as a tether for GSVs (Stockli *et al.*, 2011), it is possible that another previously characterized module that enables GIV to remodel the cortical actin cytoskeleton further aids in GSV exocytosis and glucose uptake (Enomoto *et al.*, 2005; Ghosh *et al.*, 2010). Thus, it is likely that many of GIV's modules, not just its C-terminal GEF motif, may play a role in integrating signaling events with vesicular trafficking and cytoskeletal changes to orchestrate glucose uptake after insulin stimulation.

Selective modulation of GIV-GEF emerges as a therapeutic strategy for reversal of IR

We found that cell-penetrable GIV peptides were as effective as TZDs in their ability to reverse fatty acid–induced IR in a GEF-dependent way, and activation of Gαi via GIV's GEF thus mimics the action and matches the potency of TZDs. Because postprandial lipotoxicity can also suppress GIV expression in skeletal muscles (Supplemental Figure S6), our results using cell-permeant peptides suggest that replenishing GIV-CT (with active GEF) by gene therapy may be a viable strategy for the treatment of IR. Other strategies include agonists of GIV's GEF function, antagonists of the inhibitory phospho event on GIV triggered by PKCθ, or activation of phosphatases that dephosphorylate GIV—all approaches that may serve as more refined, effective, and precise therapeutic strategies to reverse IR in skeletal muscle. GIV expressed in adipocytes is also likely to enhance the metabolic insulin response in adipose tissue, the second major site of IR. However, phosphoinhibition of GIV-GEF by PKCθ is unlikely to be a trigger for IR, because this kinase is undetectable in adipocytes (Fleming *et al.*, 1998). Instead, mechanisms such as transcriptional repression, single nucleotide polymorphisms (SNPs), or posttranslational modifications (splice variants) that reduce the levels of full-length GIV may play a role. Further studies are required to determine how IR is triggered in adipocytes and whether the GIV-targeted approaches we show here can reverse IR also in the adipose tissue.

In conclusion, we have defined activation of Gαi by GIV's GEF function as a central node that coordinately enhances the physiological insulin response and how its deregulation heralds IR. Because this node also serves as the point of convergence for the antagonistic actions of fatty acids and insulin sensitizers, selective modulation of this node emerges as a promising and precise strategy to treat T2DM and other conditions in which IR plays a central pathophysiological role.

MATERIALS AND METHODS

Detailed methods are presented in the Supplemental Materials.

Cell culture, transfection, IB, immunofluorescence, and protein–protein interaction assays

These assays were carried out exactly as described before (Ghosh *et al.*, 2008, 2010). All Odyssey images were processed using ImageJ software (National Institutes of Health [NIH], Bethesda, MD) and were assembled for presentation using Photoshop and Illustrator software (Adobe Systems, San Jose, CA).

dSTORM and FRET imaging

Direct Stochastic Optical Reconstruction Microscopy imaging was performed to reveal the interaction endogenous Gαi3 and active InsRβ at molecular level (Huang *et al.*, 2010). Control short hairpin RNA (shRNA) and GIV shRNA Cos7 stable cells were starved and stimulated with 100 nM insulin and stained with anti-Gαi3 (1:30; Calbiochem, San Diego, CA) and phospho-InsRβ antibodies (1:100; Santa Cruz Biotechnologies, Dallas, TX).

FRET assays were performed using the intracellular phosphorylation biosensors custom (phocus-2nes) designed by Yoshio Umezawa's group at the University of Tokyo (Sato *et al.*, 2002). GIV shRNA Cos7 stable cells were transfected with phocus-2nes and GIV-WT-FLAG or GIV-S1689D-FLAG. Cells were starved and stimulated with insulin and were stained with anti-FLAG antibody following the standard immunofluorescence protocol.

Patient samples

Biopsies of vastus lateralis muscle used for GIV phosphorylation analysis were collected in the Special Diagnostic and Treatment Unit of the Veterans Affairs Medical Center (San Diego, CA) and the General Clinical Research Center, University of California, San Diego (UCSD). Muscle samples were collected from healthy, normal, cycling women or women with PCOS before and after a course of treatment with Pio (45 mg/d, for 6 mo; Aroda *et al.*, 2009). Collection and storage of muscle samples and measurement of eGDR were performed as described previously (Thorburn *et al.*, 1990). The experimental protocol was approved by the Human Research Protection Program of the UCSD.

Data analysis and statistics

All experiments were repeated at least three times, and results were presented either as one representative experiment or as mean ± SD or SEM. Statistical significance was assessed with the two-tailed Student's *t* test.

ACKNOWLEDGMENTS

We thank Marilyn Farquhar, Gordon Gill, Alan Saltiel, and Jerry Olefsky (UCSD) for thoughtful comments along the way and during the preparation of this article and Kersi Pestonjamas for assistance with dSTORM microscopy at UCSD Moore's Cancer Center Microscopy Shared Facility (supported by NIH Grant P30 CA23100). This work was funded by the NIH (R01CA160911) and

the Burroughs Wellcome Fund (CAMS award to P.G.). G.S.M. was supported by the Doris Duke Charitable Foundation (DDCF grant 2013073 to P.G.) and I.L.-S. by a fellowship from the American Heart Association (AHA 14POST20050025). T.P.C. and R.R.H. were supported by grants from the American Diabetes Association and the Medical Research Service, Department of Veterans Affairs, VA San Diego Healthcare System (R.R.H.). N.K. was supported by a Cancer Cell Biology Training Grant from the National Cancer Institute (5T32CA067754-17).

REFERENCES

- Altiock S, Xu M, Spiegelman BM (1997). PPAR γ induces cell cycle withdrawal: inhibition of E2F/DP DNA-binding activity via down-regulation of PP2A. *Genes Dev* 11, 1987–1998.
- Anderson K, Fitzgerald M, Dupont M, Wang T, Paz N, Dorsch M, Healy A, Xu Y, Ocain T, Schopf L, et al. (2006). Mice deficient in PKC θ demonstrate impaired in vivo T cell activation and protection from T cell-mediated inflammatory diseases. *Autoimmunity* 39, 469–478.
- Aroda VR, Ciaraldi TP, Burke P, Mudaliar S, Clopton P, Phillips S, Chang RJ, Henry RR (2009). Metabolic and hormonal changes induced by pioglitazone in polycystic ovary syndrome: a randomized, placebo-controlled clinical trial. *J Clin Endocrinol Metab* 94, 469–476.
- Bai L, Wang Y, Fan J, Chen Y, Ji W, Qu A, Xu P, James DE, Xu T (2007). Dissecting multiple steps of GLUT4 trafficking and identifying the sites of insulin action. *Cell Metab* 5, 47–57.
- Beas AO, Taupin V, Teodorof C, Nguyen LT, Garcia-Marcos M, Farquhar MG (2012). G α s promotes EEA1 endosome maturation and shuts down proliferative signaling through interaction with GIV (Girdin). *Mol Biol Cell* 23, 4623–4634.
- Carter AM (2005). Inflammation, thrombosis and acute coronary syndromes. *Diabetes Vasc Dis Res* 2, 113–121.
- Chen JF, Guo JH, Moxham CM, Wang HY, Malbon CC (1997). Conditional, tissue-specific expression of Q205L G α i2 in vivo mimics insulin action. *J Mol Med (Berl)* 75, 283–289.
- Cho DH, Choi YJ, Jo SA, Ryou J, Kim JY, Chung J, Jo I (2006). Troglitazone acutely inhibits protein synthesis in endothelial cells via a novel mechanism involving protein phosphatase 2A-dependent p70 S6 kinase inhibition. *Am J Physiol Cell Physiol* 291, C317–C326.
- Ciaraldi TP, Maisel A (1989). Role of guanine nucleotide regulatory proteins in insulin stimulation of glucose transport in rat adipocytes. Influence of bacterial toxins. *Biochem J* 264, 389–396.
- Dunkel Y, Ong A, Notani D, Mittal Y, Lam M, Mi X, Ghosh P (2012). STAT3 protein up-regulates G α -interacting vesicle-associated protein (GIV)/Girdin expression, and GIV enhances STAT3 activation in a positive feedback loop during wound healing and tumor invasion/metastasis. *J Biol Chem* 287, 41667–41683.
- Eck MJ, Dhe-Paganon S, Trub T, Nolte RT, Shoelson SE (1996). Structure of the IRS-1 PTB domain bound to the juxtamembrane region of the insulin receptor. *Cell* 85, 695–705.
- Enomoto A, Murakami H, Asai N, Morone N, Watanabe T, Kawai K, Murakumo Y, Usukura J, Kaibuchi K, Takahashi M (2005). Akt/PKB regulates actin organization and cell motility via Girdin/APE. *Dev Cell* 9, 389–402.
- Fleming I, MacKenzie SJ, Vernon RG, Anderson NG, Houslay MD, Kilgour E (1998). Protein kinase C isoforms play differential roles in the regulation of adipocyte differentiation. *Biochem J* 333, 719–727.
- Flores-Riveros JR, Sibley E, Kastelic T, Lane MD (1989). Substrate phosphorylation catalyzed by the insulin receptor tyrosine kinase. Kinetic correlation to autophosphorylation of specific sites in the beta subunit. *J Biol Chem* 264, 21557–21572.
- Garcia-Marcos M, Ear J, Farquhar MG, Ghosh P (2011). A GDI (AGS3) and a GEF (GIV) regulate autophagy by balancing G protein activity and growth factor signals. *Mol Biol Cell* 22, 673–686.
- Garcia-Marcos M, Ghosh P, Ear J, Farquhar MG (2010). A structural determinant that renders G α ph(i) sensitive to activation by GIV/girdin is required to promote cell migration. *J Biol Chem* 285, 12765–12777.
- Garcia-Marcos M, Ghosh P, Farquhar MG (2009). GIV is a nonreceptor GEF for G α i with a unique motif that regulates Akt signaling. *Proc Natl Acad Sci USA* 106, 3178–3183.
- Garcia-Marcos M, Ghosh P, Farquhar MG (2015). GIV/Girdin transmits signals from multiple receptors by triggering trimeric G protein activation. *J Biol Chem* 290, 6697–6704.
- Ghosh P, Beas AO, Bornheimer SJ, Garcia-Marcos M, Forry EP, Johansson C, Ear J, Jung BH, Cabrera B, Carethers JM, Farquhar MG (2010). A G α i-GIV molecular complex binds epidermal growth factor receptor and determines whether cells migrate or proliferate. *Mol Biol Cell* 21, 2338–2354.
- Ghosh P, Garcia-Marcos M, Bornheimer SJ, Farquhar MG (2008). Activation of G α i3 triggers cell migration via regulation of GIV. *J Cell Biol* 182, 381–393.
- Gohla A, Klement K, Nurnberg B (2007). The heterotrimeric G protein G(i3) regulates hepatic autophagy downstream of the insulin receptor. *Autophagy* 3, 393–395.
- Goodyear LJ, Giorgino F, Sherman LA, Carey J, Smith RJ, Dohm GL (1995). Insulin receptor phosphorylation, insulin receptor substrate-1 phosphorylation, and phosphatidylinositol 3-kinase activity are decreased in intact skeletal muscle strips from obese subjects. *J Clin Invest* 95, 2195–2204.
- Griffin ME, Marcucci MJ, Cline GW, Bell K, Barucci N, Lee D, Goodyear LJ, Kraegen EW, White MF, Shulman GI (1999). Free fatty acid-induced insulin resistance is associated with activation of protein kinase C θ and alterations in the insulin signaling cascade. *Diabetes* 48, 1270–1274.
- Haasch D, Berg C, Clampitt JE, Pederson T, Frost L, Kroeger P, Rondinone CM (2006). PKC θ is a key player in the development of insulin resistance. *Biochem Biophys Res Commun* 343, 361–368.
- Hartung A, Ordelheide AM, Staiger H, Melzer M, Haring HU, Lammers R (2013). The Akt substrate Girdin is a regulator of insulin signaling in myoblast cells. *Biochim Biophys Acta* 1833, 2803–2811.
- Hoehn KL, Hohnen-Behrens C, Cederberg A, Wu LE, Turner N, Yuasa T, Ebina Y, James DE (2008). IRS1-independent defects define major nodes of insulin resistance. *Cell Metab* 7, 421–433.
- Huang B, Babcock H, Zhuang X (2010). Breaking the diffraction barrier: super-resolution imaging of cells. *Cell* 143, 1047–1058.
- Hwang H, Bowen BP, Lefort N, Flynn CR, De Filippis EA, Roberts C, Smoke CC, Meyer C, Hojlund K, Yi Z, Mandarino LJ (2010). Proteomics analysis of human skeletal muscle reveals novel abnormalities in obesity and type 2 diabetes. *Diabetes* 59, 33–42.
- Imamura T, Vollenweider P, Egawa K, Clodi M, Ishibashi K, Nakashima N, Ugi S, Adams JW, Brown JH, Olefsky JM (1999). G α q/11 protein plays a key role in insulin-induced glucose transport in 3T3-L1 adipocytes. *Mol Cell Biol* 19, 6765–6774.
- Itani SI, Zhou Q, Pories WJ, MacDonald KG, Dohm GL (2000). Involvement of protein kinase C in human skeletal muscle insulin resistance and obesity. *Diabetes* 49, 1353–1358.
- Kahn BB, Flier JS (2000). Obesity and insulin resistance. *J Clin Invest* 106, 473–481.
- Kanoh Y, Ishizuka T, Morita H, Ishizawa M, Miura A, Kajita K, Kimura M, Suzuki T, Sakuma H, Yasuda K (2000). Effect of pertussis toxin on insulin-induced signal transduction in rat adipocytes and soleus muscles. *Cell Signal* 12, 223–232.
- Kim JK, Fillmore JJ, Sunshine MJ, Albrecht B, Higashimori T, Kim DW, Liu ZX, Soos TJ, Cline GW, O'Brien WR, et al. (2004). PKC- θ knockout mice are protected from fat-induced insulin resistance. *J Clin Invest* 114, 823–827.
- Knowlden JM, Jones HE, Barrow D, Gee JM, Nicholson RI, Hutcheson IR (2008). Insulin receptor substrate-1 involvement in epidermal growth factor receptor and insulin-like growth factor receptor signalling: implication for Gefitinib (“Iressa”) response and resistance. *Breast Cancer Res Treat* 111, 79–91.
- Kreuzer J, Nurnberg B, Krieger-Brauer HI (2004). Ligand-dependent autophosphorylation of the insulin receptor is positively regulated by Gi-proteins. *Biochem J* 380, 831–836.
- Krook AK, Moller DE, Dib K, O'Rahilly S (1996). Two naturally occurring mutant insulin receptors phosphorylate insulin receptor substrate-1 (IRS-1) but fail to mediate the biological effects of insulin. Evidence that IRS-1 phosphorylation is not sufficient for normal insulin action. *J Biol Chem* 271, 7134–7140.
- Krupinski J, Rajaram R, Lakonishok M, Benovic JL, Cerione RA (1988). Insulin-dependent phosphorylation of GTP-binding proteins in phospholipid vesicles. *J Biol Chem* 263, 12333–12341.
- Lansey MN, Walker NN, Hargett SR, Stevens JR, Keller SR (2012). Deletion of Rab GAP AS160 modifies glucose uptake and GLUT4 translocation in primary skeletal muscles and adipocytes and impairs glucose homeostasis. *Am J Physiol Endocrinol Metab* 303, E1273–E1286.
- Le-Niculescu H, Niesman I, Fischer T, DeVries L, Farquhar MG (2005). Identification and characterization of GIV, a novel G α ph α i/s-interacting protein found on COPI, endoplasmic reticulum-Golgi transport vesicles. *J Biol Chem* 280, 22012–22020.

- Le Roith D, Zick Y (2001). Recent advances in our understanding of insulin action and insulin resistance. *Diabetes Care* 24, 588–597.
- Leto D, Saltiel AR (2012). Regulation of glucose transport by insulin: traffic control of GLUT4. *Nat Rev Mol Cell Biol* 13, 383–396.
- Li Y, Soos TJ, Li X, Wu J, Degennaro M, Sun X, Littman DR, Birnbaum MJ, Polakiewicz RD (2004). Protein kinase C θ inhibits insulin signaling by phosphorylating IRS1 at Ser(1101). *J Biol Chem* 279, 45304–45307.
- Lin C, Ear J, Midde K, Lopez-Sanchez I, Aznar N, Garcia-Marcos M, Kufareva I, Abagyan R, Ghosh P (2014). Structural basis for activation of trimeric Gi proteins by multiple growth factor receptors via GIV/Girdin. *Mol Biol Cell* 25, 3654–3671.
- Lin C, Ear J, Pavlova Y, Mittal Y, Kufareva I, Ghassemian M, Abagyan R, Garcia-Marcos M, Ghosh P (2011). Tyrosine phosphorylation of the G α -interacting protein GIV promotes activation of phosphoinositide 3-kinase during cell migration. *Sci Signal* 4, ra64.
- Lin X, O'Mahony A, Mu Y, Gelezunas R, Greene WC (2000). Protein kinase C- θ participates in NF- κ B activation induced by CD3-CD28 costimulation through selective activation of I κ B kinase β . *Mol Cell Biol* 20, 2933–2940.
- Lo IC, Gupta V, Midde KK, Taupin V, Lopez-Sanchez I, Kufareva I, Abagyan R, Randazzo PA, Farquhar MG, Ghosh P (2015). Activation of G α i at the Golgi by GIV/Girdin imposes finiteness in Arf1 signaling. *Dev Cell* 33, 189–203.
- Lopez-Sanchez I, Dunkel Y, Roh YS, Mittal Y, De Minicis S, Muranyi A, Singh S, Shanmugam K, Aroonsakool N, Murray F, et al. (2014). GIV/Girdin is a central hub for profibrogenic signalling networks during liver fibrosis. *Nat Commun* 5, 4451.
- Lopez-Sanchez I, Garcia-Marcos M, Mittal Y, Aznar N, Farquhar MG, Ghosh P (2013). Protein kinase C- θ (PKC θ) phosphorylates and inhibits the guanine exchange factor, GIV/Girdin. *Proc Natl Acad Sci USA* 110, 5510–5515.
- Ma GS, Aznar N, Kalogiropoulos N, Midde KK, Lopez-Sanchez I, Sato E, Dunkel Y, Gallo RL, Ghosh P (2015). Therapeutic effects of cell-permeant peptides that activate G proteins downstream of growth factors. *Proc Natl Acad Sci USA* 112, E2602–E2610.
- Maegawa H, Shigeta Y, Egawa K, Kobayashi M (1991). Impaired autophosphorylation of insulin receptors from abdominal skeletal muscles in nonobese subjects with NIDDM. *Diabetes* 40, 815–819.
- Markova I, Zidek V, Musilova A, Simakova M, Mlejnek P, Kazdova L, Pravenec M (2010). Long-term pioglitazone treatment augments insulin sensitivity and PKC- ϵ and PKC- θ activation in skeletal muscles in sucrose fed rats. *Physiol Res* 59, 509–516.
- Mashili F, Chibalin AV, Krook A, Zierath JR (2013). Constitutive STAT3 phosphorylation contributes to skeletal muscle insulin resistance in type 2 diabetes. *Diabetes* 62, 457–465.
- Midde KK, Aznar N, Laederich MB, Ma GS, Kunkel MT, Newton AC, Ghosh P (2015). Multimodular biosensors reveal a novel platform for activation of G proteins by growth factor receptors. *Proc Natl Acad Sci USA* 112, E937–E946.
- Miinea CP, Sano H, Kane S, Sano E, Fukuda M, Peranen J, Lane WS, Lienhard GE (2005). AS160, the Akt substrate regulating GLUT4 translocation, has a functional Rab GTPase-activating protein domain. *Biochem J* 391, 87–93.
- Moxham CM, Malbon CC (1996). Insulin action impaired by deficiency of the G-protein subunit G α_{i2} . *Nature* 379, 840–844.
- Myers MG Jr, Grammer TC, Brooks J, Glasheen EM, Wang LM, Sun XJ, Blenis J, Pierce JH, White MF (1995). The pleckstrin homology domain in insulin receptor substrate-1 sensitizes insulin signaling. *J Biol Chem* 270, 11715–11718.
- Nolan JJ, Freidenberg G, Henry R, Reichart D, Olefsky JM (1994). Role of human skeletal muscle insulin receptor kinase in the in vivo insulin resistance of noninsulin-dependent diabetes mellitus and obesity. *J Clin Endocrinol Metab* 78, 471–477.
- O'Brien RM, Houslay MD, Milligan G, Siddle K (1987). The insulin receptor tyrosyl kinase phosphorylates holomeric forms of the guanine nucleotide regulatory proteins Gi and Go. *FEBS Lett* 212, 281–288.
- Pessin JE, Saltiel AR (2000). Signaling pathways in insulin action: molecular targets of insulin resistance. *J Clin Invest* 106, 165–169.
- Pugazhenthis S, Khandelwal RL (1998). Insulin action on protein phosphatase-1 activation is enhanced by the antidiabetic agent pioglitazone in cultured diabetic hepatocytes. *Mol Cell Biochem* 182, 185–191.
- Rothenberg PL, Kahn CR (1988). Insulin inhibits pertussis toxin-catalyzed ADP-ribosylation of G-proteins. Evidence for a novel interaction between insulin receptors and G-proteins. *J Biol Chem* 263, 15546–15552.
- Rundek T, Gardener H, Xu Q, Goldberg RB, Wright CB, Boden-Albala B, Disla N, Paik MC, Elkind MS, Sacco RL (2010). Insulin resistance and risk of ischemic stroke among nondiabetic individuals from the northern Manhattan study. *Arch Neurol* 67, 1195–1200.
- Saltiel AR, Kahn CR (2001). Insulin signalling and the regulation of glucose and lipid metabolism. *Nature* 414, 799–806.
- Sato M, Ozawa T, Inukai K, Asano T, Umezawa Y (2002). Fluorescent indicators for imaging protein phosphorylation in single living cells. *Nat Biotechnol* 20, 287–294.
- Schmitz-Peiffer C, Browne CL, Oakes ND, Watkinson A, Chisholm DJ, Kraegen EW, Biden TJ (1997). Alterations in the expression and cellular localization of protein kinase C isozymes epsilon and theta are associated with insulin resistance in skeletal muscle of the high-fat-fed rat. *Diabetes* 46, 169–178.
- Sharma C, Pradeep A, Pestell RG, Rana B (2004). Peroxisome proliferator-activated receptor gamma activation modulates cyclin D1 transcription via beta-catenin-independent and cAMP-response element-binding protein-dependent pathways in mouse hepatocytes. *J Biol Chem* 279, 16927–16938.
- Shulman GI (2000). Cellular mechanisms of insulin resistance. *J Clin Invest* 106, 171–176.
- Song X, Zheng X, Malbon CC, Wang H (2001). G α_{i2} enhances in vivo activation of and insulin signaling to GLUT4. *J Biol Chem* 276, 34651–34658.
- Stockli J, Fazakerley DJ, James DE (2011). GLUT4 exocytosis. *J Cell Sci* 124, 4147–4159.
- Sun Y, Bilan PJ, Liu Z, Klip A (2010). Rab8A and Rab13 are activated by insulin and regulate GLUT4 translocation in muscle cells. *Proc Natl Acad Sci USA* 107, 19909–19914.
- Sun XJ, Rothenberg P, Kahn CR, Backer JM, Araki E, Wilden PA, Cahill DA, Goldstein BJ, White MF (1991). Structure of the insulin receptor substrate IRS-1 defines a unique signal transduction protein. *Nature* 352, 73–77.
- Taniguchi CM, Emanuelli B, Kahn CR (2006). Critical nodes in signalling pathways: insights into insulin action. *Nat Rev Mol Cell Biol* 7, 85–96.
- Thorburn AW, Gumbiner B, Bulacan F, Wallace P, Henry RR (1990). Intracellular glucose oxidation and glycogen synthase activity are reduced in non-insulin-dependent (type II) diabetes independent of impaired glucose uptake. *J Clin Invest* 85, 522–529.
- Uhlen M, Oksvold P, Fagerberg L, Lundberg E, Jonasson K, Forsberg M, Zwahlen M, Kampf C, Wester K, Hober S, et al. (2010). Towards a knowledge-based Human Protein Atlas. *Nat Biotechnol* 28, 1248–1250.
- Voliovitch H, Schindler DG, Hadari YR, Taylor SI, Accili D, Zick Y (1995). Tyrosine phosphorylation of insulin receptor substrate-1 in vivo depends upon the presence of its pleckstrin homology region. *J Biol Chem* 270, 18083–18087.
- Weng L, Enomoto A, Miyoshi H, Takahashi K, Asai N, Morone N, Jiang P, An J, Kato T, Kuroda K, et al. (2014). Regulation of cargo-selective endocytosis by dynamin 2 GTPase-activating protein girdin. *EMBO J* 33, 2098–2112.
- White MF (2006). Regulating insulin signaling and beta-cell function through IRS proteins. *Canadian J Physiol Pharmacol* 84, 725–737.
- White MF, Shoelson SE, Keutmann H, Kahn CR (1988). A cascade of tyrosine autophosphorylation in the beta-subunit activates the phosphotransferase of the insulin receptor. *J Biol Chem* 263, 2969–2980.
- Wunderlich CM, Hovelmeyer N, Wunderlich FT (2013). Mechanisms of chronic JAK-STAT3-SOCS3 signaling in obesity. *Jak-Stat* 2, e23878.
- Yamamoto N, Sato T, Kawasaki K, Murosaki S, Yamamoto Y (2006). A non-radioisotope, enzymatic assay for 2-deoxyglucose uptake in L6 skeletal muscle cells cultured in a 96-well microplate. *Analytical Biochem* 351, 139–145.
- Yu C, Chen Y, Cline GW, Zhang D, Zong H, Wang Y, Bergeron R, Kim JK, Cushman SW, Cooney GJ, et al. (2002). Mechanism by which fatty acids inhibit insulin activation of insulin receptor substrate-1 (IRS-1)-associated phosphatidylinositol 3-kinase activity in muscle. *J Biol Chem* 277, 50230–50236.